TFAWS Active Thermal Paper Session

Flow Boiling and Condensation Experiment: Flow Boiling in a Rectangular Channel with Subcooled Inlet Conditions in Microgravity

Henry Nahra[1], R. Balasubramaniam[4], Mohammad Hasan[1], Jeff Mackey[2], Issam Mudawar[3], V.S. Devahdhanush[3], Steven J. Darges[3], Rochelle May[1], Nancy Hall[1]

[1]NASA Glenn Research Center, 21000 Brookpark Rd., Cleveland, OH 44135,
[2]HX5, LLC, 3000 Aerospace Parkway, Brook Park, OH 44142, USA
[3]Purdue University Boiling and Two-Phase Flow Laboratory (PU-BTFPL), 585 Purdue Mall, West Lafayette, IN 47907, U.S.A
[4]Case Western Reserve University, 10900 Euclid Ave., Cleveland, OH 44106, USA

THERMAL & FLUIDS ANALYSIS WORKSHOP

TFAWS

GSFC · 2023

FBCE
NASA Glenn Research Center
Purdue University
μg
FLOW BOILING AND CONDENSATION EXPERIMENT

Presented By
Henry K. Nahra, Ph.D.
FBCE Project Scientist

Thermal & Fluids Analysis Workshop
TFAWS 2023
August 21-25, 2023
NASA Goddard Space Flight Center
Greenbelt, MD

Presentation Content

- Experiment Overview
- FBCE Science Objective
- Top Level Science Requirements and Constraints
- Fluid System Description
- Flow Boiling Module
- Experimental Results
  - Interfacial Two-phase Flow structures
  - Flow boiling heat transfer

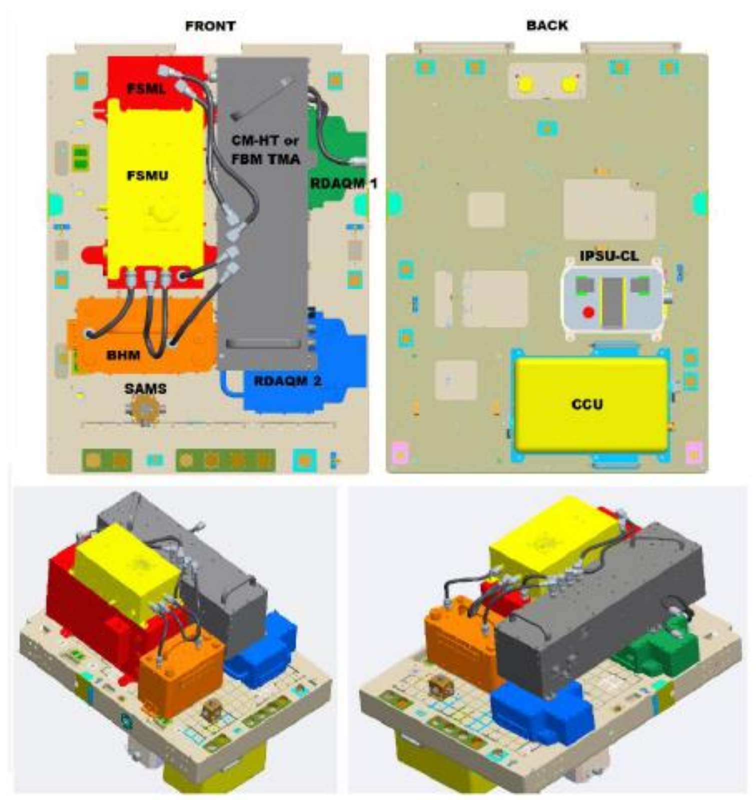

FBCE – Experiment Overview

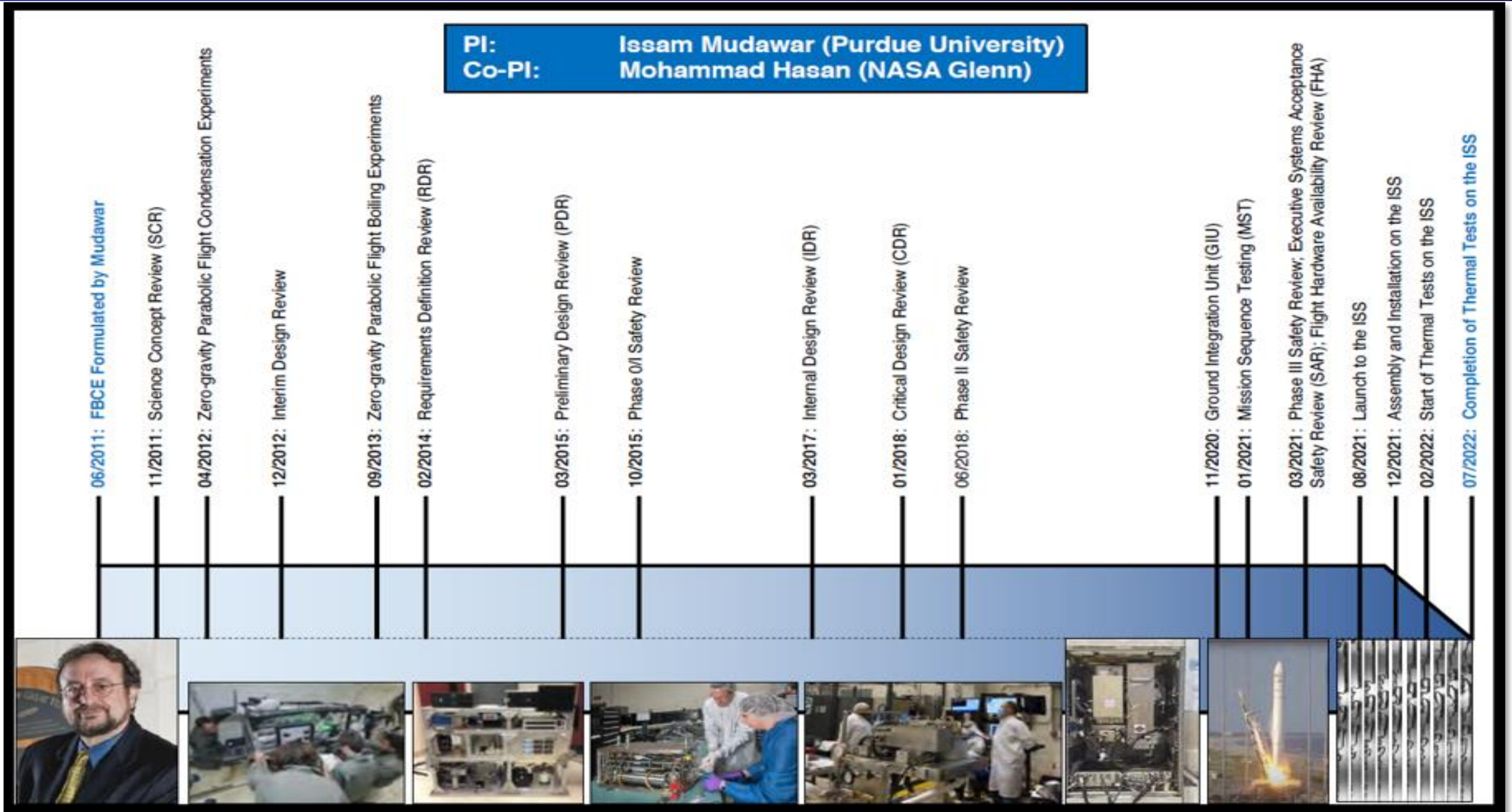

From a presentation made by Prof. Issam Mudawar, ASGSR Conference, 2022

- The proposed research aims to develop *an integrated two-phase flow boiling/condensation facility for the International Space Station (ISS)* to serve as primary platform for obtaining two-phase flow and heat transfer data in microgravity.

Key objectives are:

- Develop experimentally validated, **mechanistic model** for microgravity flow boiling **critical heat flux (CHF)** and **dimensionless criteria** to predict **minimum flow velocity** required to ensure **gravity-independent CHF**
- Develop experimentally validated, **mechanistic model** for microgravity annular condensation and **dimensionless criteria** to predict **minimum flow velocity** required to ensure **gravity-independent annular condensation**; also develop correlations for other condensation regimes in microgravity

Applications of FBCE include:

- Rankine Cycle Power Conversion System for Space
- Two Phase Flow Thermal Control Systems and Advanced Life Support Systems
- Gravity Insensitive Vapor Compression Heat Pump for Future Space Vehicles and Planetary Bases
- Cryogenic Liquid Storage and Transfer

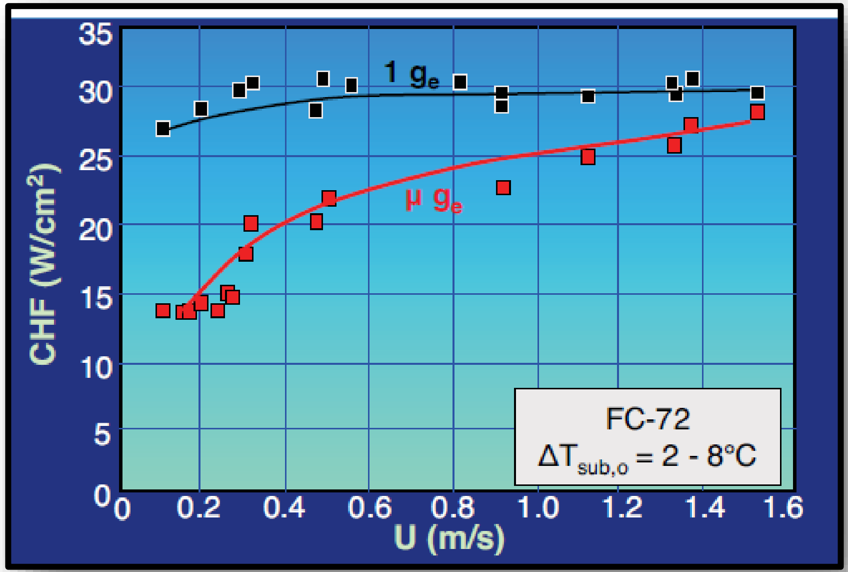

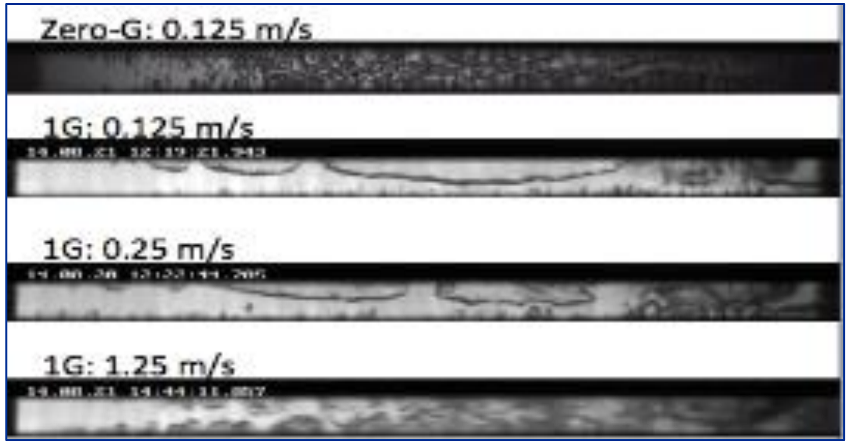

FBCE Hardware on Fluid System Schematic

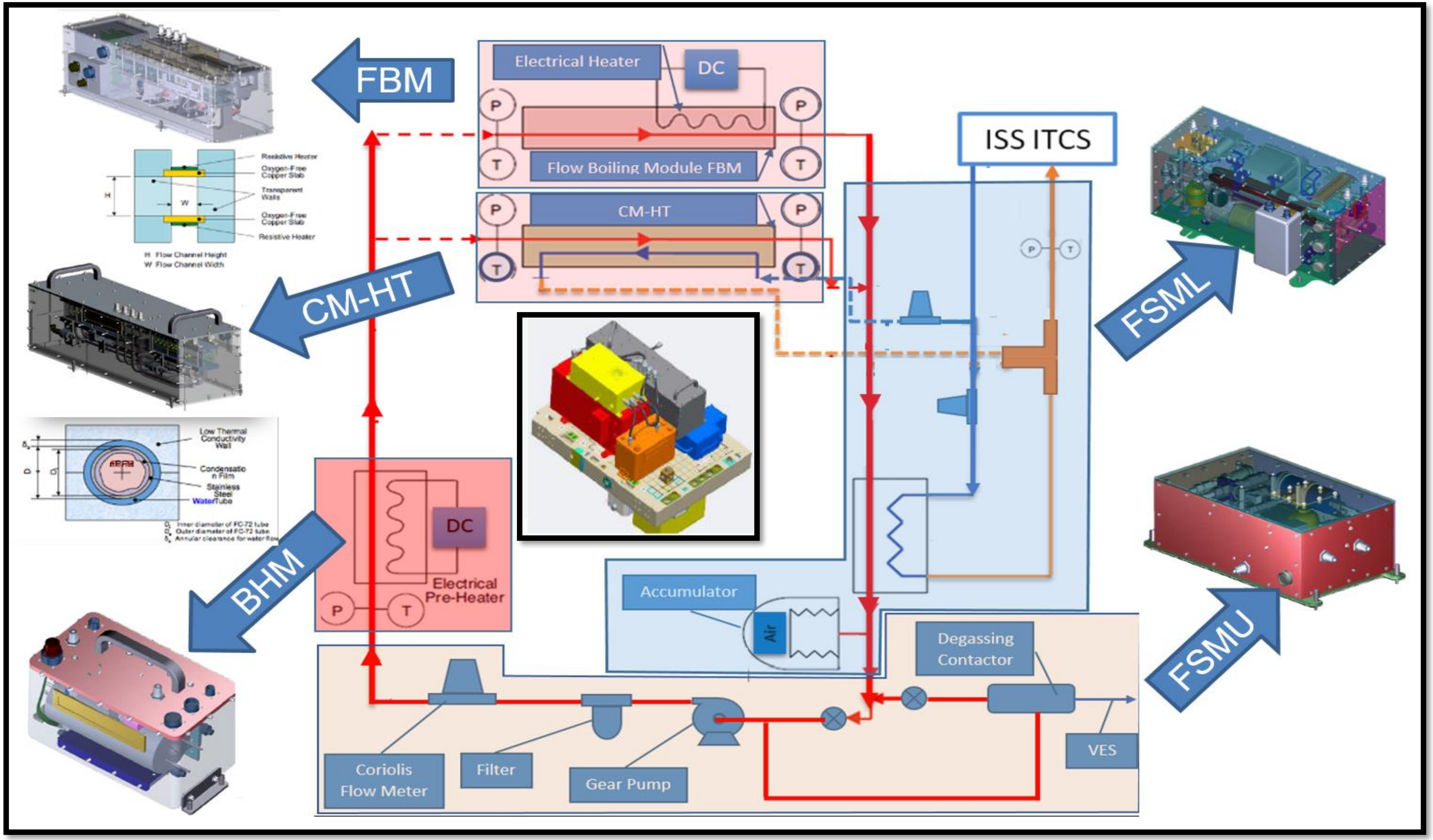

Top Level Science Requirements and Constraints

• Fluid System Capability

- Delivers flow rates between 2 and 14 g/s of nPFH for Condensation Experiments and 2 to 40 g/s for Flow Boiling Experiments
- Delivers up to 1440 W to the fluid from the bulk heater and 340 W from the FBM heater
- Delivers a system pressure of 130 to 160 kPa
- Volume increase is accommodated with an accumulator
- Delivers the required thermodynamic conditions of the fluid at the entrance of the test modules (subcooled, saturated and two-phase mixture)
- Provides the fluid cooling function via ISS ITCS cooling water
- Provides degassing function for the test fluid

• Constraints

- Limitation on the available power
- ITCS cooling water flow rate up ~50 g/s to and returning stream temperature requirement of 40-49 °C
- Volume constraint 91.44×121.92×48.28 cm^3 (36×48×19 in^3)

FBCE in the Fluid Integrated Rack

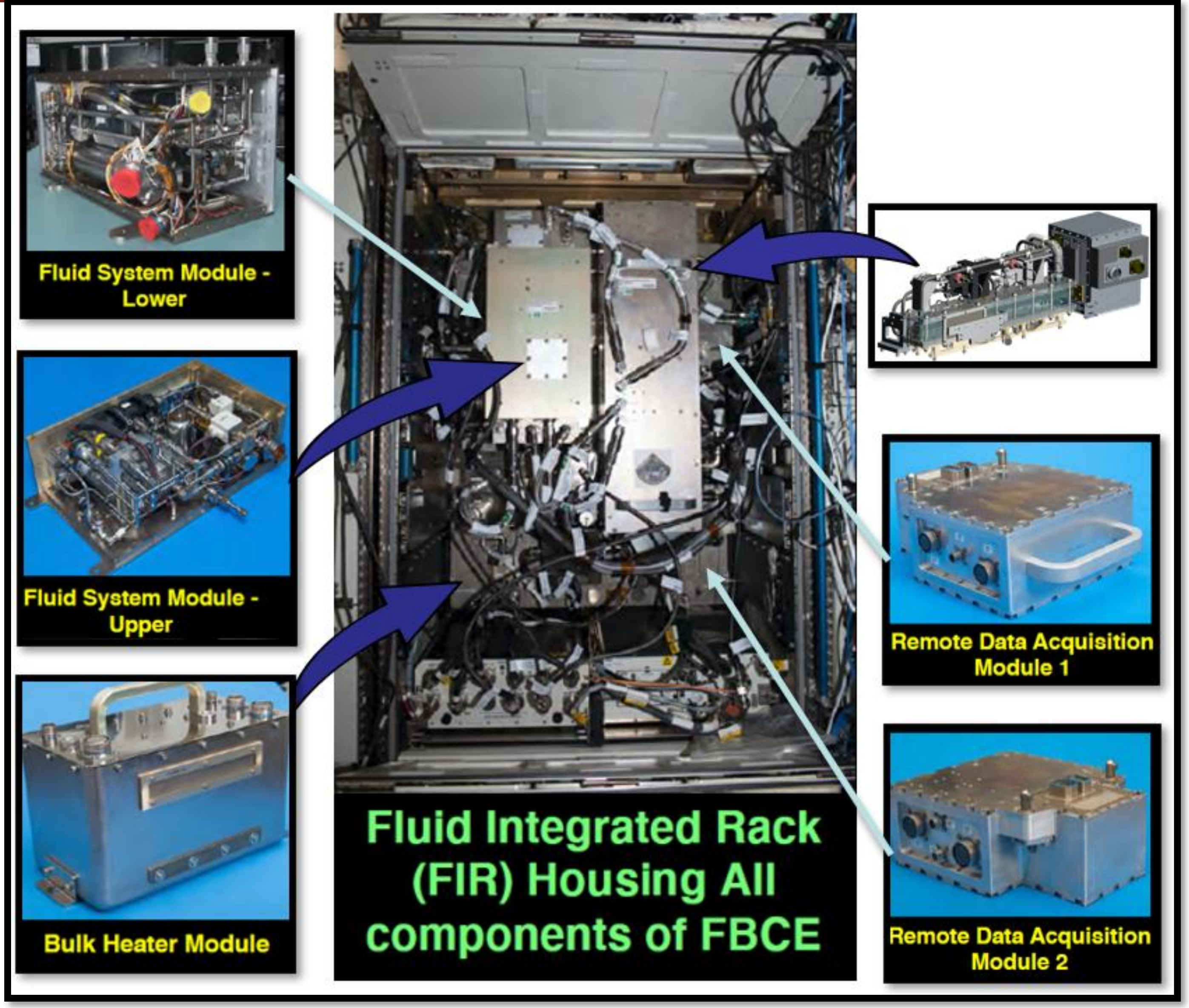

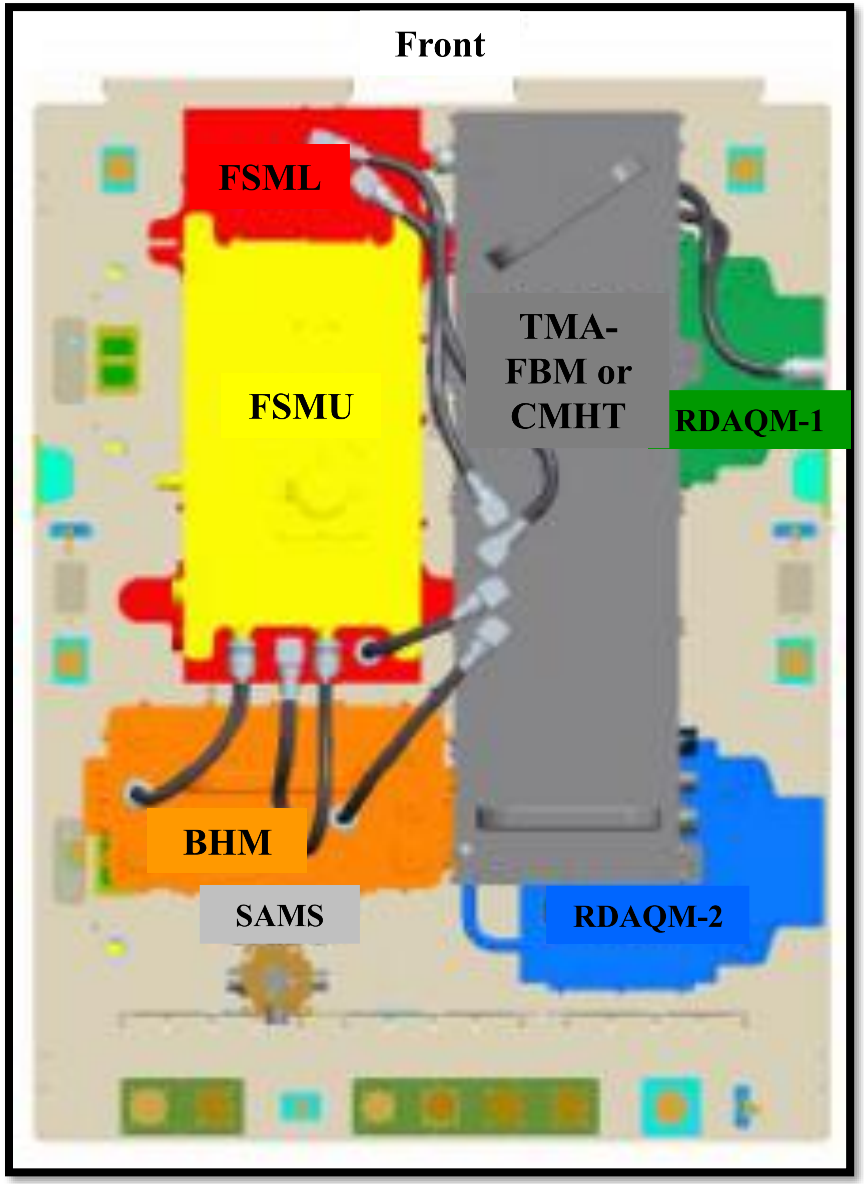

The Flow Boiling Module

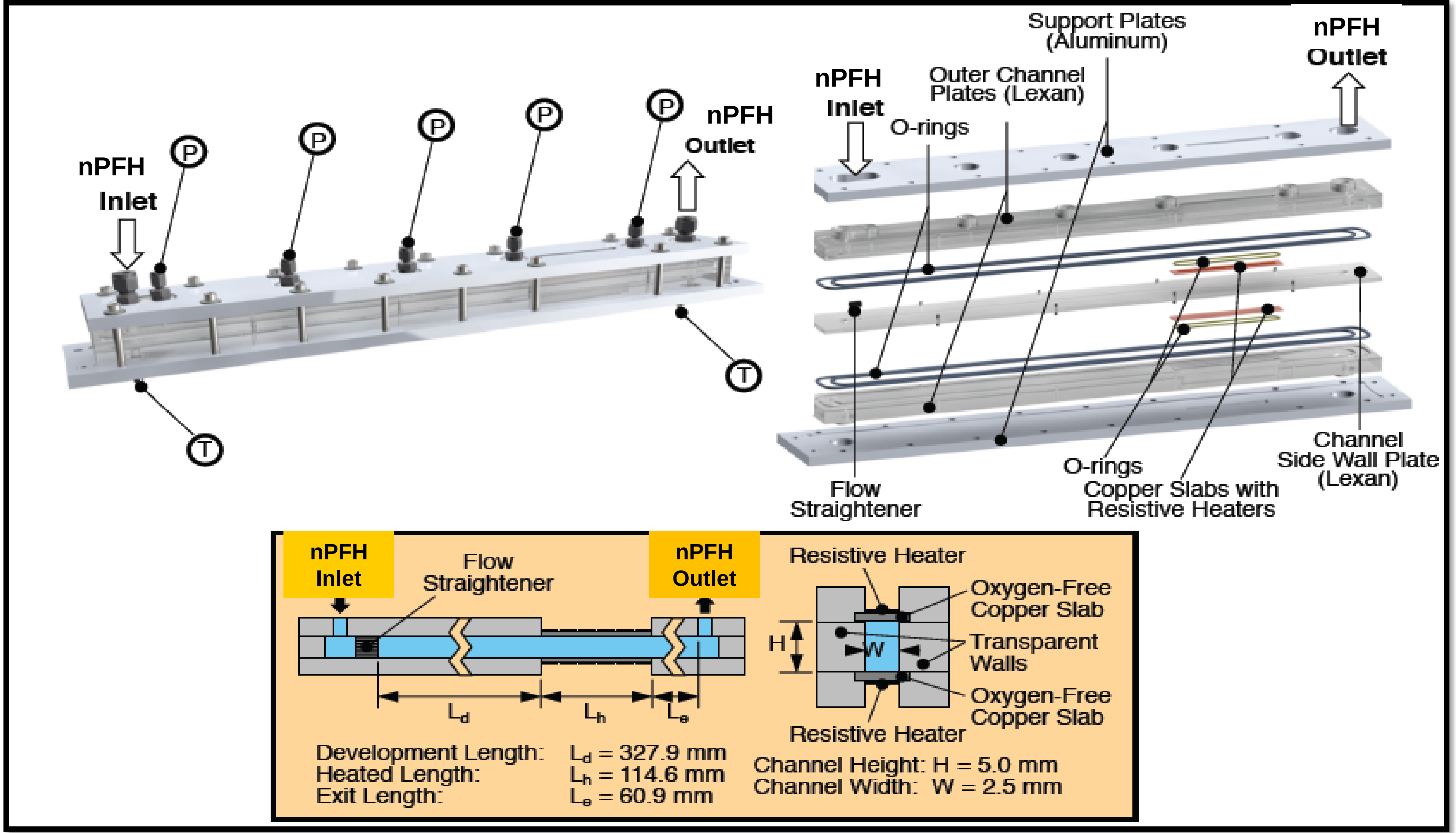

More on the Flow Boiling Module

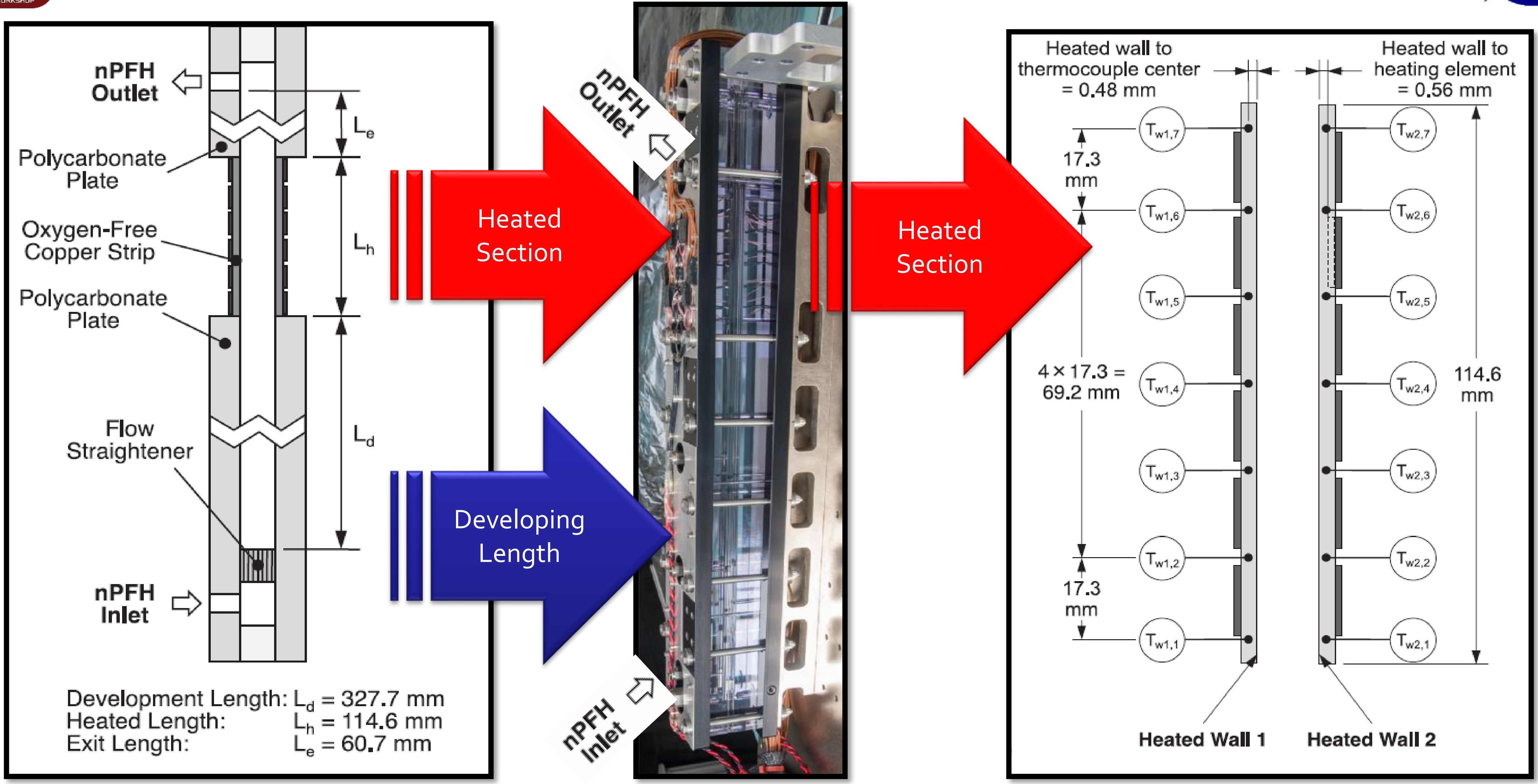

Flow Visualization/Imaging

- Analysis of the interfacial physics of flow boiling is possible by flow visualization using high-speed video photography of all heat flux increments from a minimum until (and including) CHF.
- Visualization enabled by transparent polycarbonate wall on FBM
- Transparent polycarbonate allows for excellent visual access to within the FBM's heated section.
- All three plates were further vapor polished to minimize vignetting effects produced by the opaque copper strips and O-rings.
- CMOS sensor, each pixel of which is a square of size 5.5 μm ×5.5 μm.
- The CMOS sensor has a fill factor of 100%, *i.e* ., the pixels are arranged with no physical distance between them.
- Spatial resolution of at least ~90 μm was achieved

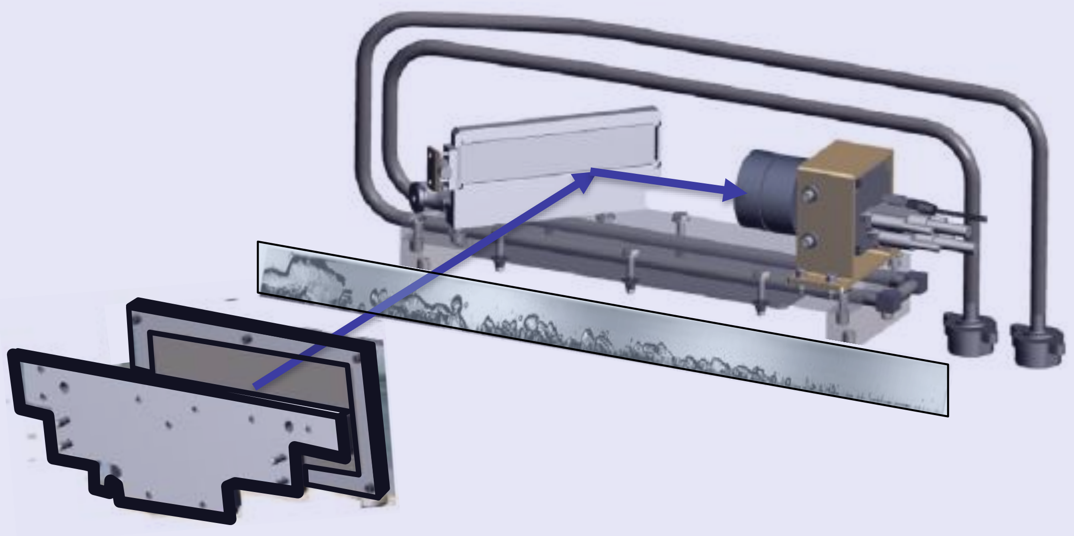

High-Speed Video Camera and Mirror

- High-speed video camera is pointed at one of the transparent channel walls with a channel height of H = 5.0 mm
- Opposite channel wall is backlit with blue light emitting diodes (LEDs) in tandem with a light-shaping diffuser fitted with an intermediate Teflon sheet which is necessary due to the extremely short light transmission distance

Flight Experimental Procedure

- Experiments performed via commanding from NASA-GRC Telescience Center
- Parameters like desired pressure, inlet temperature, bulk heater power, FBM power, flow rates of nPFH and water were obtained from the Experiment Parameter Master Table (EPMT)
- EPMT was uploaded to ISS and test points parameters can be taken directly from the EPMT (Run by ID) or uploaded individually (Run by Parameter)

test Number	test Matrix Number	npfh FlowRate	fbm Heater Increment DelayTime	max Waiting Time	module Water FlowRate	condenser Water FlowRate	module Inlet Temperature	saturation Temperature	subcooling	quality	mass Velocity	module Inlet Pressure	bulk Heater Aux Power	num BulkHeater Cartridges 120/23C	bulk Heater Temperature	fbm Heaters Enabled	fbm Heater Power1	fbm Heater Power2	fbm Heater Power3	fbm Heater Power4	fbm Heater Power5	fbm Heater Power6	fbm Heater Power7	fbm Heater Power8	fbm Heater Power9	fbm Heater Power10	fbm Heater Power11	fbm Heater Power12
1	I-01	2.50	0.00	120.00	4.00	30.00	63.30	65.30	2.00	0.00	200.00	18.85	181.00	0	70.30	3.00	4.00	8.52	13.03	17.55	22.07	26.58	31.10	35.62	40.13	44.65	49.17	50.42
2	I-02	4.00	0.00	120.00	4.00	30.00	63.30	65.30	2.00	0.00	320.00	18.85	181.00	1	70.30	3.00	4.00	9.10	14.19	19.29	24.38	29.48	34.58	39.67	44.77	49.86	54.96	56.21
3	I-03	6.00	0.00	120.00	4.00	30.00	63.30	65.30	2.00	0.00	480.00	18.85	181.00	1	70.30	3.00	4.00	9.61	15.23	20.84	26.45	32.07	37.68	43.29	48.91	54.52	60.13	61.38
4	I-04	8.00	0.00	120.00	4.00	30.00	63.30	65.30	2.00	0.00	640.00	18.85	181.00	1	70.30	3.00	4.00	10.01	16.03	22.04	28.06	34.07	40.09	46.10	52.12	58.13	64.15	65.40
5	I-05	10.00	0.00	120.00	4.00	30.00	63.30	65.30	2.00	0.00	800.00	18.85	181.00	1	70.30	3.00	4.00	10.33	16.65	22.98	29.30	35.63	41.95	48.28	54.60	60.93	67.25	68.50
6	I-06	16.00	0.00	120.00	4.00	30.00	63.30	65.30	2.00	0.00	1280.00	18.85	181.00	2	70.30	3.00	4.00	10.97	17.95	24.92	31.90	38.87	45.84	52.82	59.79	66.77	73.74	74.99
7	I-07	20.00	0.00	120.00	4.00	30.00	63.30	65.30	2.00	0.00	1600.00	18.85	181.00	2	70.30	3.00	4.00	11.32	18.64	25.96	33.29	40.61	47.93	55.25	62.57	69.89	77.22	78.47
8	I-08	26.00	0.00	120.00	4.00	30.00	63.30	65.30	2.00	0.00	2080.00	18.85	181.00	3	70.30	3.00	4.00	11.75	19.50	27.25	35.00	42.75	50.50	58.25	66.00	73.75	81.50	82.75

A Flow Boiling Run

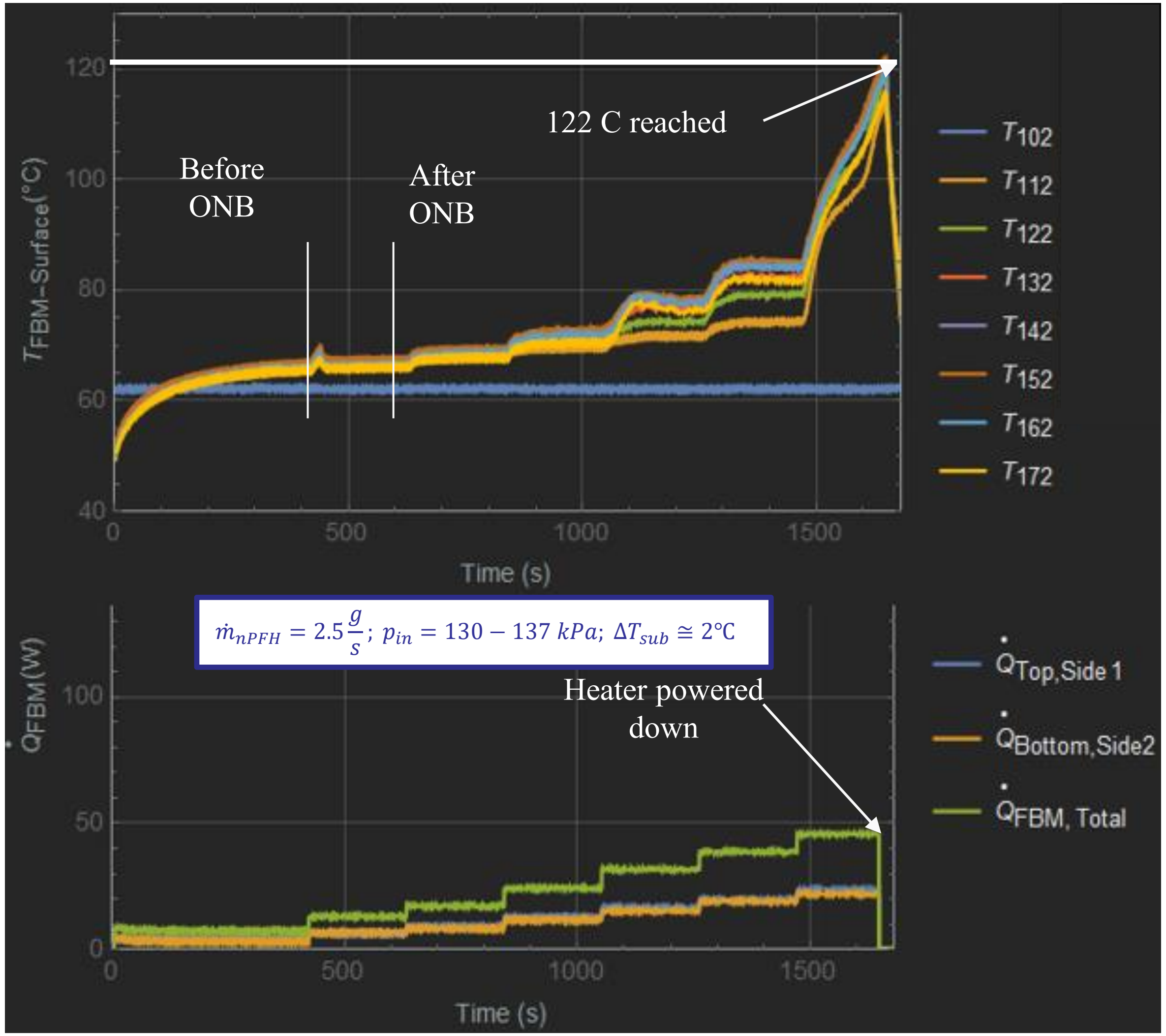

Variations of temperatures of heated surface and power for heat flux increments from a minimum to CHF

Note: No bubbles before ONB

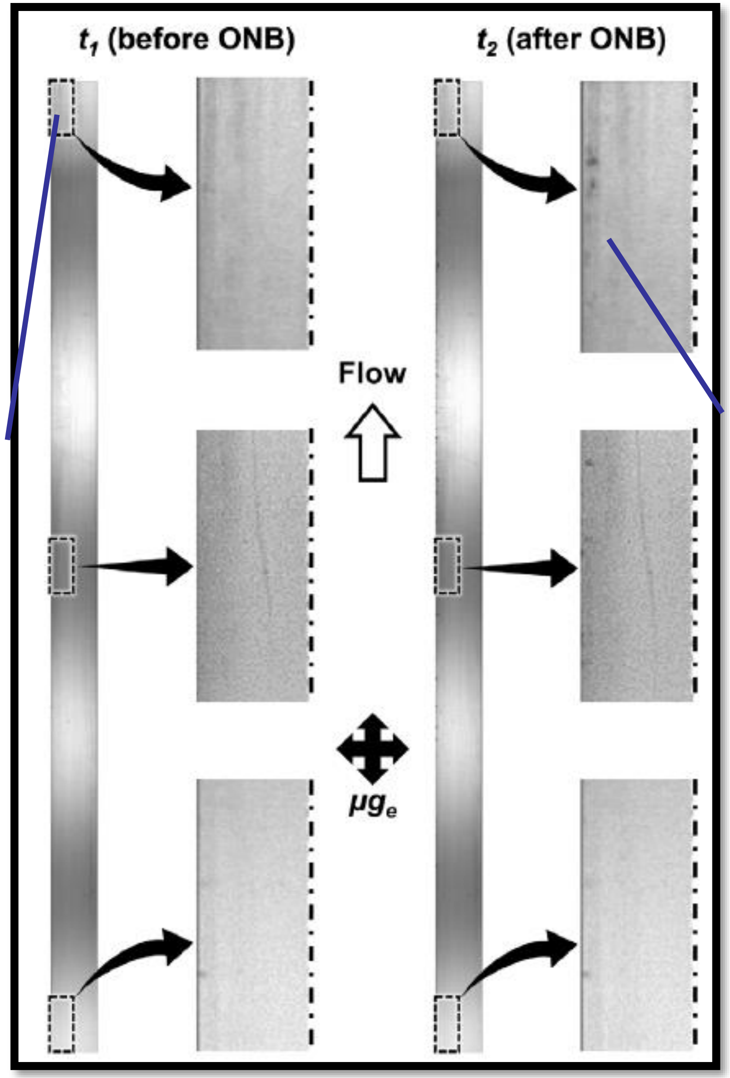

Note: Bubbles after ONB

Visualization at time instants t_1 and t_2

Flow Visualization

Imaging Types

1. Type 1 Images
   - ➢ Evolution of average flow pattern in FBM with increasing heat flux along boiling curve from ONset of Boiling (ONB) →→→→until reaching Critical Heat Flux CHF
2. Type 2 Images
   - ➢ Images sequenced over specific time interval for specific heat fluxes
     - Capture of Transients

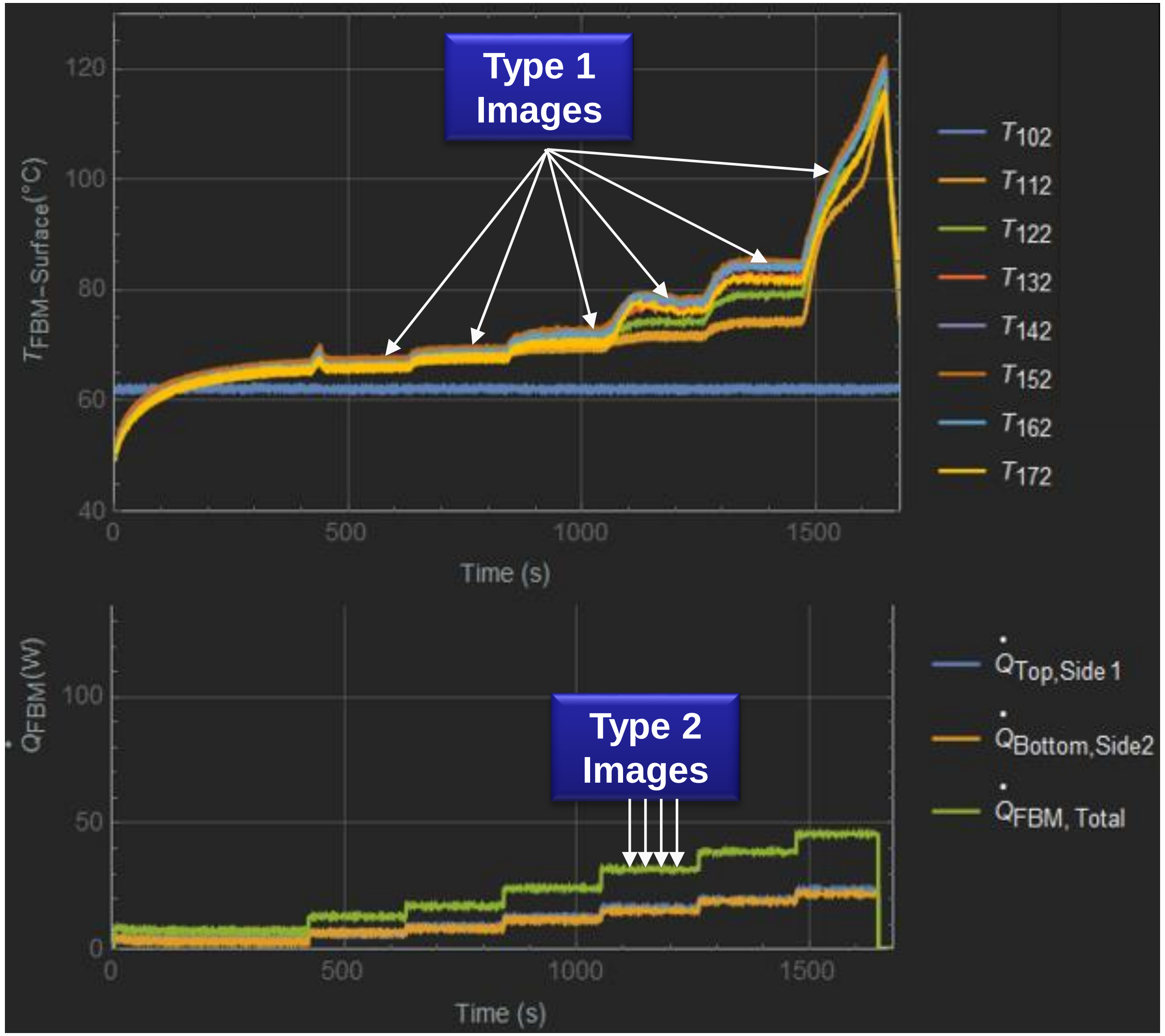

Flow Visualization-Effects of Inlet Subcooling

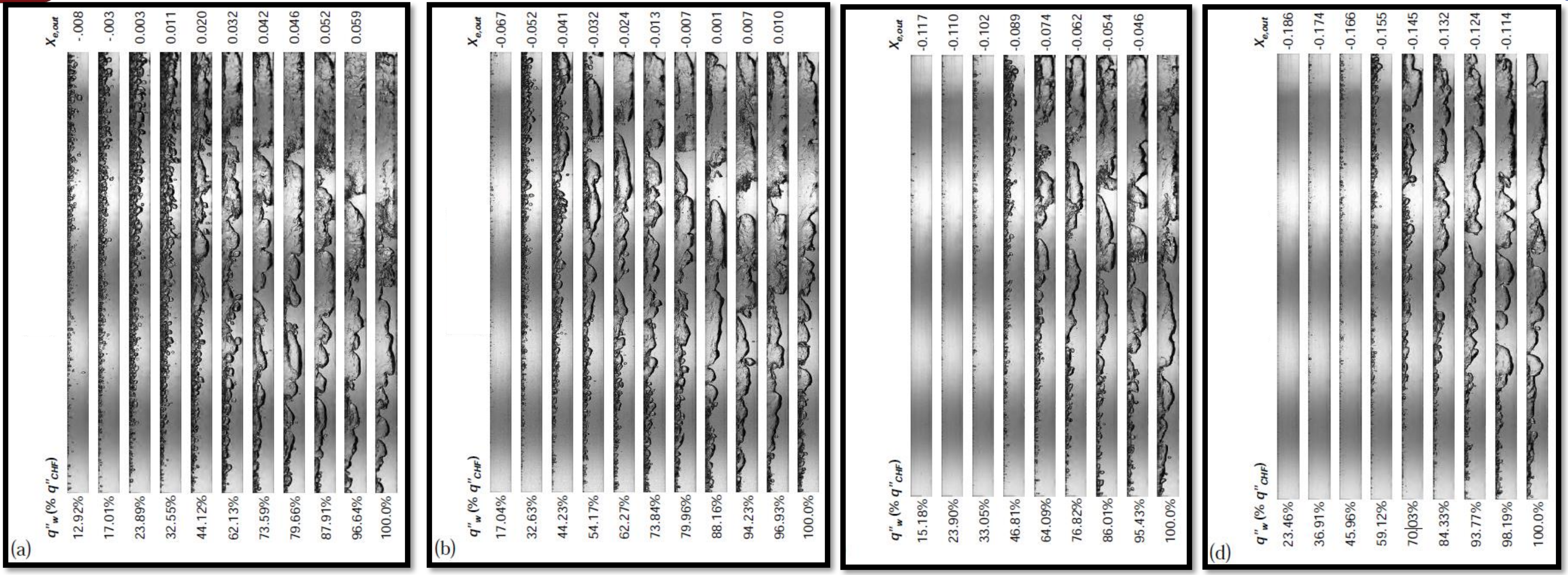

Flow Parameters: $799.96 \leq G \leq 803.13 \frac{kg}{m^2.s}$; $p_{in} \cong 150\ kPa$;

$\Delta T_{Subcool} = 2.1$ ℃	6.06 ℃	9.6℃	15 ℃
$q''_{CHF} = 25.33\ W/cm^2$	25.25	23.83	24.31

Flow Visualization-Effects of Inlet Subcooling Summary

	High Inlet Subcooling	Low Inlet Subcooling
Interfacial Flow	▪ Thinner bubble boundary layers and vapor layers. ▪ Transitions in flow regime take place further downstream and with increased heat fluxes. ▪ Bubbles are extremely small at lower heat fluxes ▪ As CHF is approached by increasing the heat flux, the vapor layer develops peaks that extend to the opposite wall of FBM. ▪ At CHF, wetting fronts are still present upstream of the heated section.	▪ Thicker bubble boundary layers and vapor layers. ▪ Transitions in flow regime take place further upstream and at lower heat fluxes. ▪ At lower heat fluxes, bubbles are larger and do coalesce. ▪ As CHF is approached by increasing the heat flux, the vapor layer almost completely occupies the channel's cross section. ▪ At CHF, wetting fronts no longer exist

Flow Visualization-Effects of Mass Flow Rate @ High $\Delta T_{Subcool}$

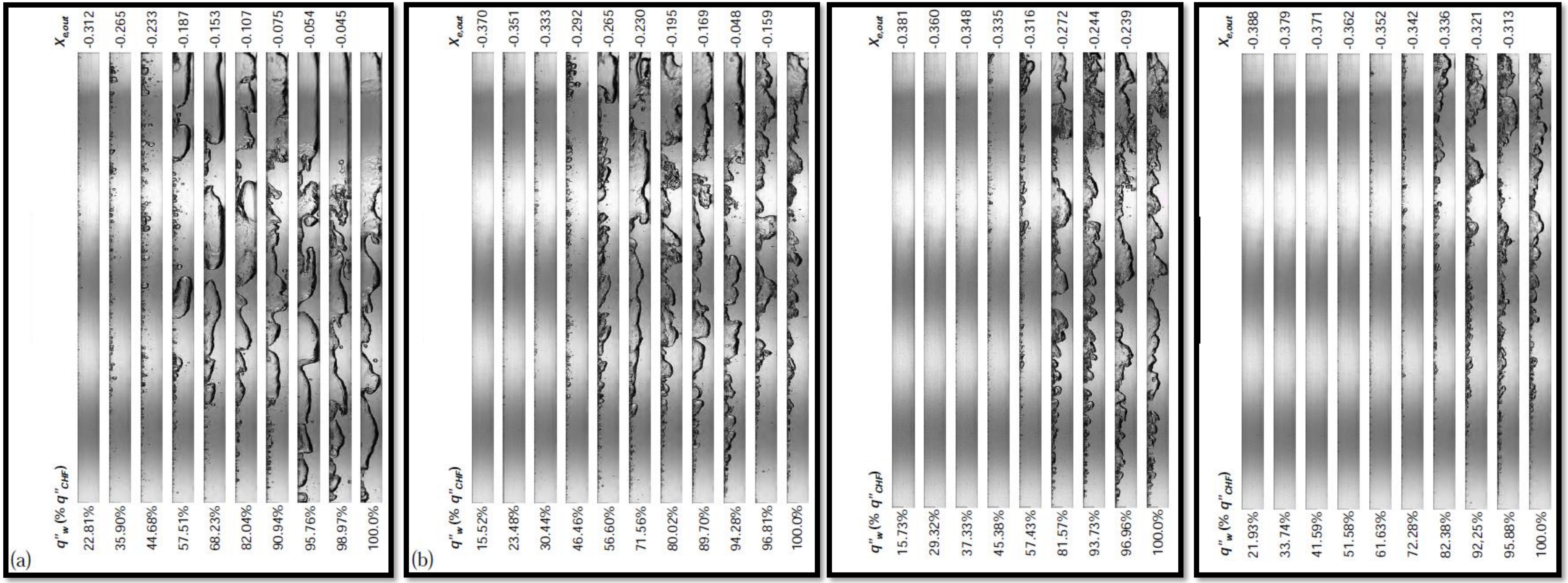

Flow Parameters: $p_{in} \cong 146 - 151\ kPa;\ \Delta T_{Subcool} \cong 29 - 30\ ℃$

$\dot{m} = 2.5\frac{g}{s}$ $5\frac{g}{s}$ $10\frac{g}{s}$ $20\frac{g}{s}$

Flow Visualization-Effects of Mass Flow Rate @ Low $\Delta T_{Subcool}$

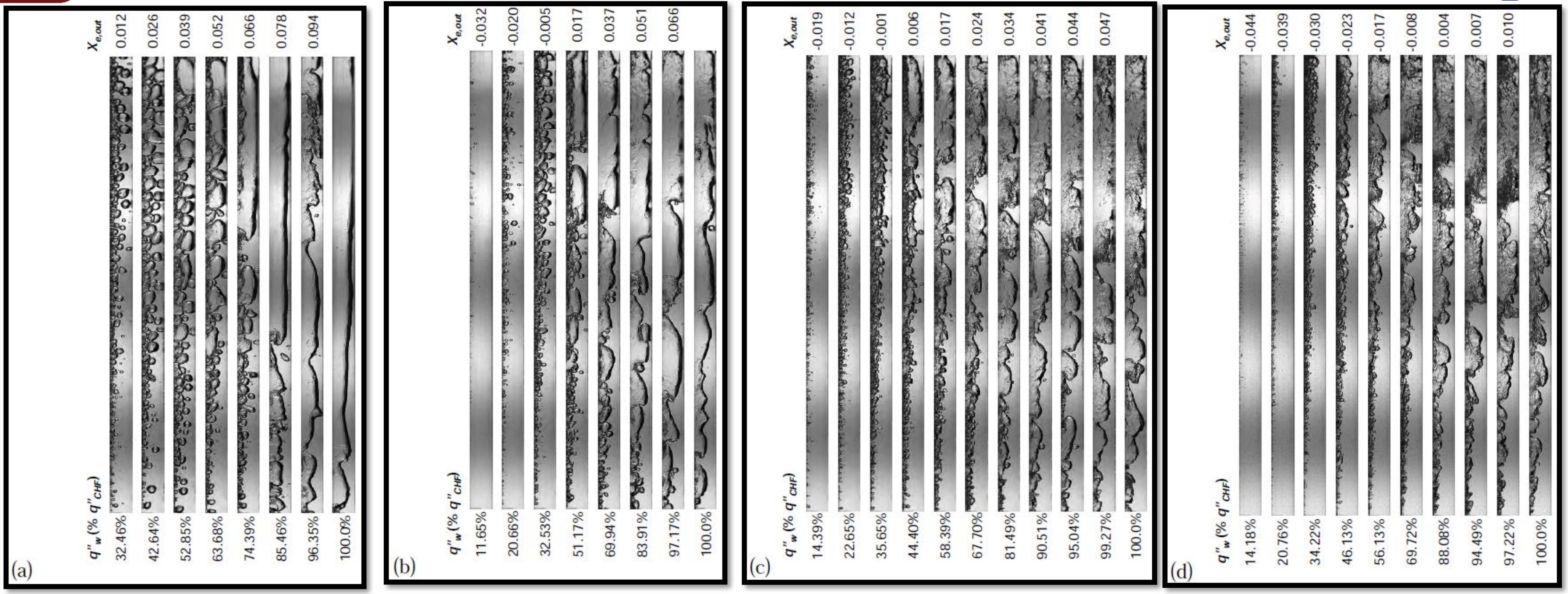

Flow Parameters: $p_{in} \cong 150 - 152\ kPa$; $\Delta T_{Subcool} \cong 3 - 4\ °C$

$\dot{m} = 2.5\,\frac{g}{s}$ $\quad \frac{5g}{s}$ $\quad 10\,\frac{g}{s}$ $\quad 20\,\frac{g}{s}$

Flow Visualization-Effects of Mass Flow Rate Summary

	Low Mass Flow Rate	High Mass Flow Rate
Interfacial Flow	▪ Thicker bubble boundary layers and vapor layers. ▪ Larger vapor structures ▪ Transitions in flow regime take place further upstream and at lower heat fluxes. ▪ At CHF with high subcooling, the heated wall is completely insulated with a continuous wavy vapor layer with absence of wetting fronts ▪ At CHF with low subcooling, the heated wall is completely embedded in a vapor layer that is continuous with a characteristically longer wavelength	▪ Thinner bubble boundary layers and vapor layers. ▪ Smaller vapor structures ▪ Transitions in flow regime take place further downstream and at higher heat fluxes. ▪ At CHF with high subcooling, a single phase region forms upstream ▪ At CHF with low subcooling, a vapor layer of smaller wavelength exists along the heated wall with reduced wetting fronts and highly turbulent interfacial structures downstream.
		
		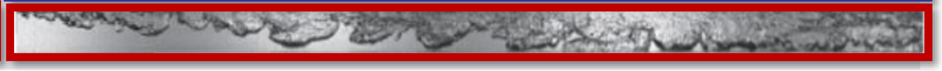

Flow Visualization Type 2-Effects of Inlet Subcooling

Observations

Lower Heat Flux

- Consistent movement and growth of the vapor patches is observed
- Wetting front is observed to slide along the heated wall in the flow direction, and new wetting fronts form upstream as the wetting front downstream leave

Higher Heat Flux

- Wavy vapor layer is shown to develop and grow in the streamwise direction with periodic wetting fronts along the heated wall.
- The growth rate and production of larger, more continuous vapor layers is accelerated by the increase heat flux
- Wetting fronts are observed to accelerate along the heated wall due to boiling within them.

G = 799.96 kg/m^{2}s, p_{in} = 153.98 kPa, T_{in} = 67.97°C, **$\Delta T_{sub,in}$ = 2.11°C**, $x_{e,in}$ = -0.029
q''_{CHF} = 25.33 W/cm^2

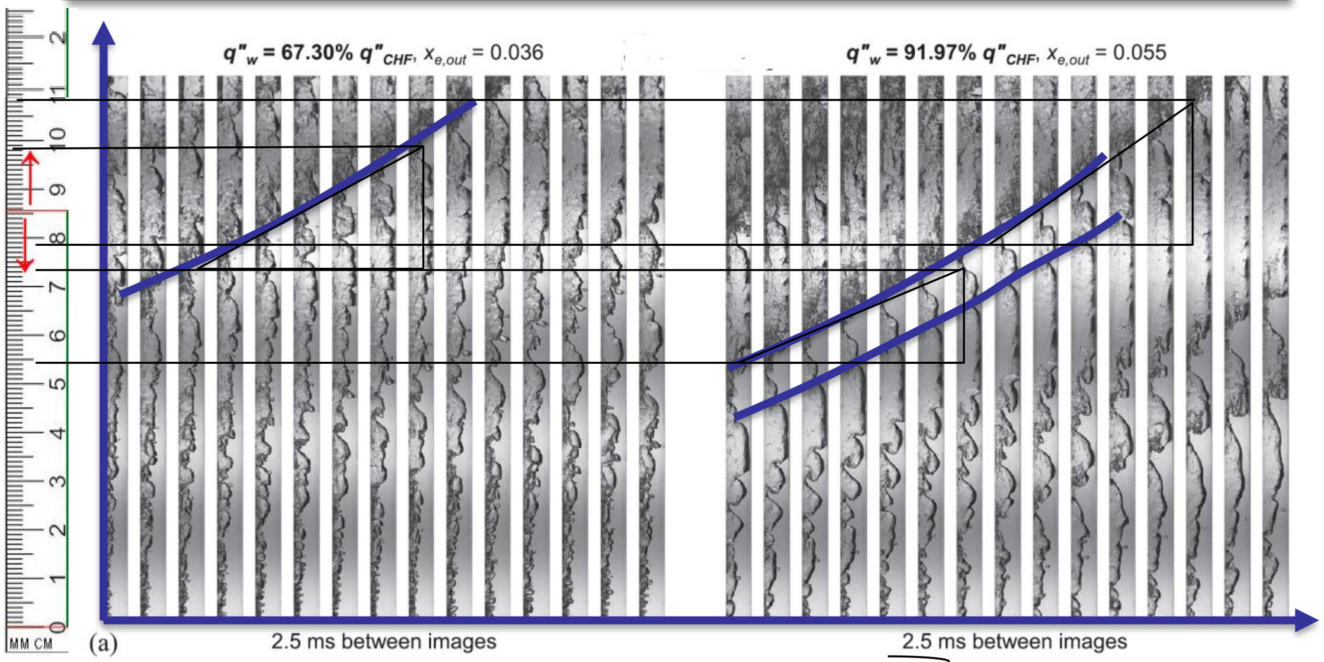

$$v = \frac{dx}{dt} \cong \frac{(107-78)mm}{6\times 2.5\ \ 10^{-3}s} \times \frac{1m}{1000\ mm} = 1.93\ m/s$$

$$v = \frac{dx}{dt} \cong \frac{(73-54)mm}{6\times 2.5\ \ 10^{-3}s} \times \frac{1m}{1000\ mm} = 1.27\ m/s$$

$$a = \frac{dv}{dt} \cong 0.033\ m/s^2$$

Note that Superficial Liquid Velocity= $\frac{\dot{m}}{\rho A} = 0.5\ m/s$

Flow Visualization Type 2-Effects of Inlet Subcooling

Observations

Lower Heat Flux

- Clear upstream single-phase length is observed followed by bubble nucleation on the heated wall
- Some bubbles condensation observed as bubbles slide downstream due to the high degree of subcooling
- Periodicity in the shape of the vapor waves is noted.

Higher Heat Flux

- Bubble nucleation occurs further upstream, and less condensation occurs as bubbles produced upstream continuously grow into the wavy vapor layers.
- Vapor grows in an alternating fashion of thicker and thinner patches
- Acceleration of fronts depend on the dynamics of the vapor structures that are downstream and upstream.

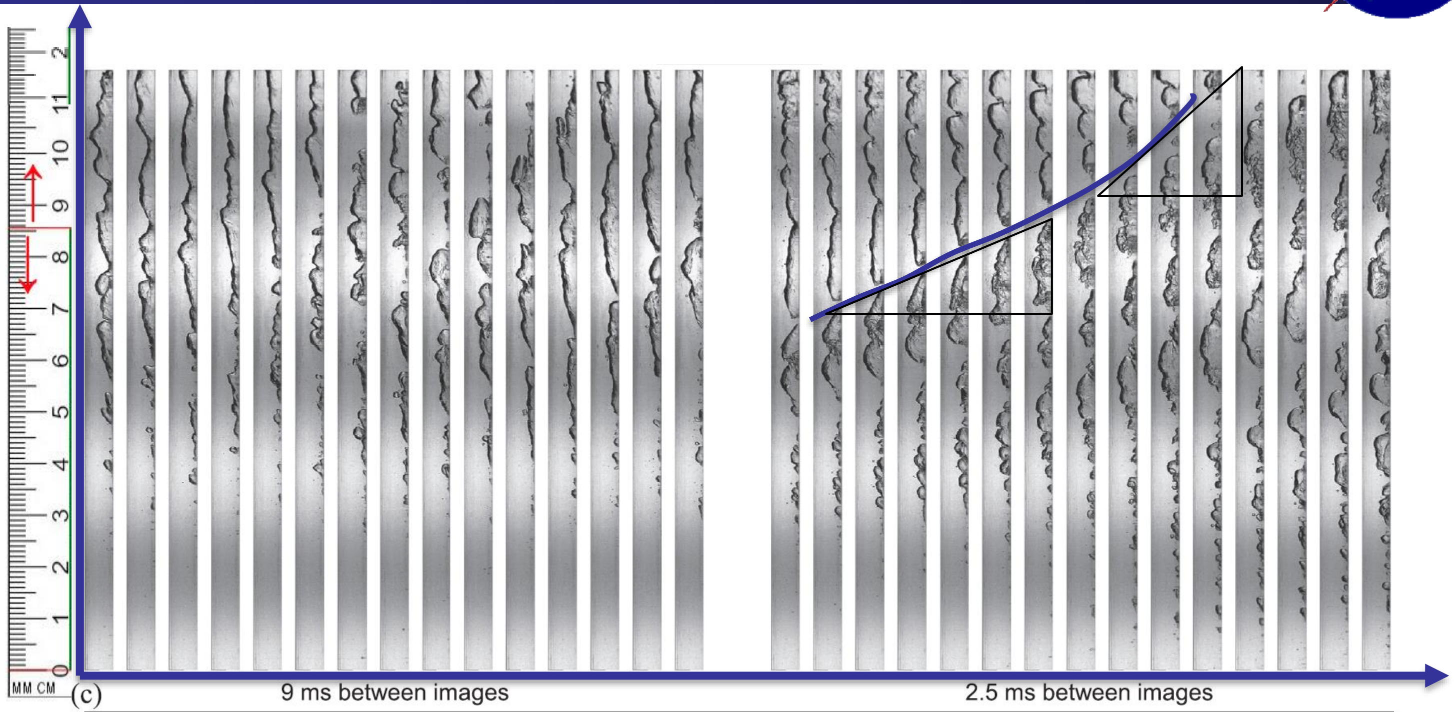

G = 801.75 kg/m²s, p_{in} = 147.40 kPa, T_{in} = 34.04°C, $\Delta T_{sub,in}$ = **34.62°C**, $x_{e,in}$ = -0.465
q''_{CHF} = 46.82 W/cm²

q''_w = 68.71% q''_{CHF}, $x_{e,out}$ = -0.348

q''_w = 85.80% q''_{CHF}, $x_{e,out}$ = -0.302

$$v = \frac{dx}{dt} \cong \frac{(86-68)mm}{5\times 2.5\ \ 10^{-3}s} \times \frac{1m}{1000\ mm} = 1.44\ m/s$$

$$v = \frac{dx}{dt} \cong \frac{(115-92)mm}{3\times 2.5\ \ 10^{-3}s} \times \frac{1m}{1000\ mm} = 3.07\ m/s$$

$$a = \frac{dv}{dt} \cong 0.093\ m/s^2$$

Quick Comparison with Mission Sequence Tests Results

Ground Observations from Mission Sequence Tests

- Vapor patches move at a more uniform/constant velocity compared to microgravity
- Vapor waves tend to move faster in 1 g vertical up-flow compared to microgravity
- Similar flow characteristics are observed in one g compared to microgravity such as
  - Thicker boundary and vapor layers at lower flow rates versus thinner ones at high flow rate

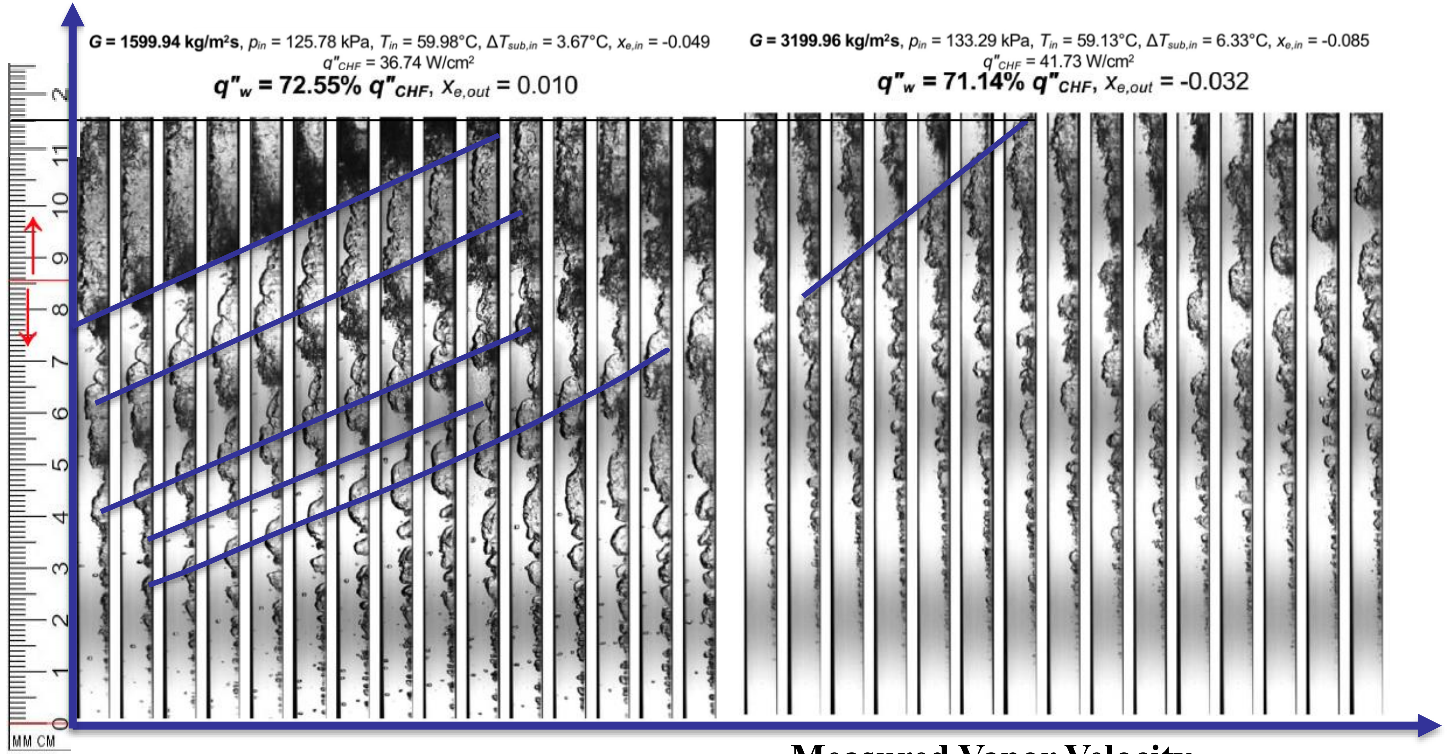

Superficial Liquid Velocity

G=1600 kg/m^2.s
1 m/s→→→→→→→→ →→→→→

G=3200 kg/m^2.s
2 m/s →→→→→→→→ →→→→→

Measured Vapor Velocity

$$v = \frac{dx}{dt} \cong \frac{(114.6 - 74)mm}{9 \times 1.5\ \ 10^{-3}s} \times \frac{1m}{1000\ mm} = 3\ m/s$$

$$v = \frac{dx}{dt} \cong \frac{(114.6 - 84)mm}{5 \times 1.5\ \ 10^{-3}s} \times \frac{1m}{1000\ mm} = 4.26\ m/s$$

Flow Oscillation and Instabilities

T_{in} = 40.26°C
$\Delta T_{sub,in}$ = 29.06°C

G = 201.45 kg/m²s
p_{in} = 148.94 kPa

10 ms between images

$x_{e,in}$ = -0.392
q''_{CHF} = 24.98 W/cm²

q''_w = 95.76% q''_{CHF}
$x_{e,out}$ = -0.054

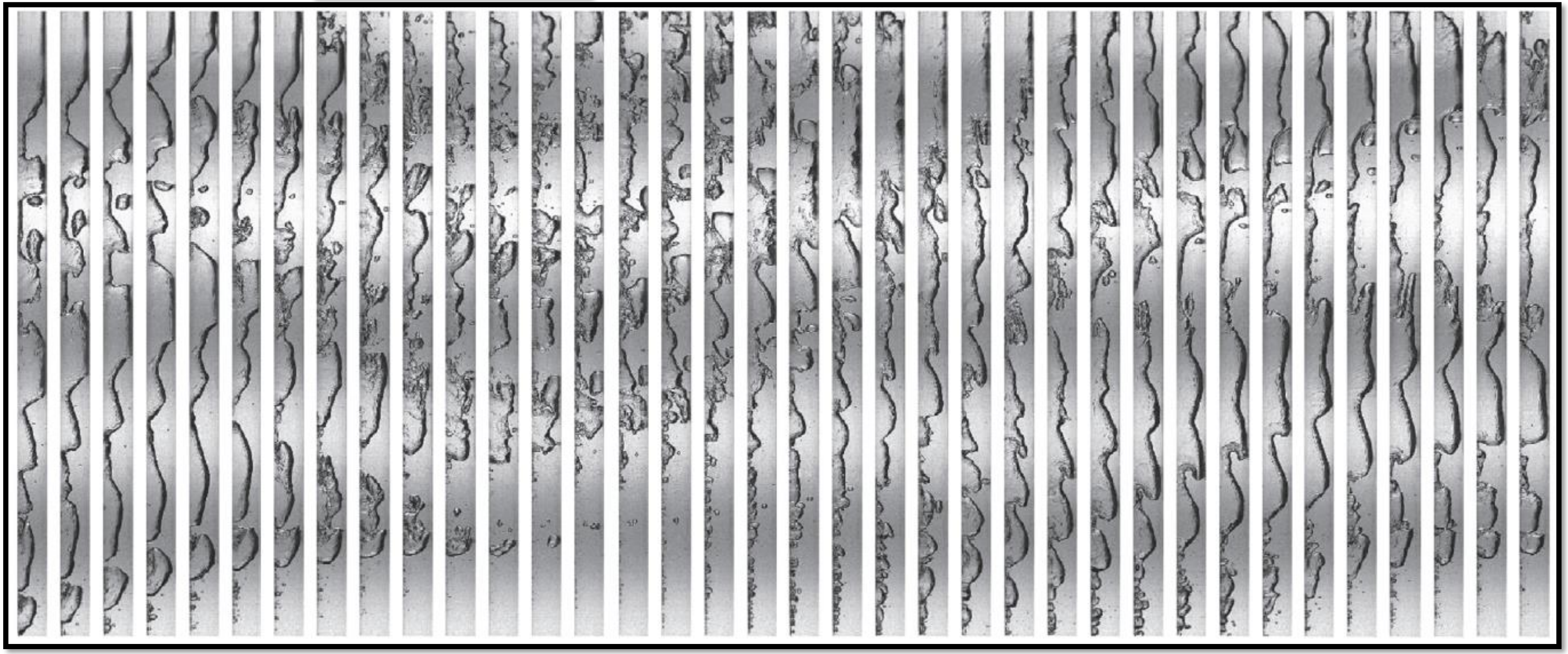

Boiling Curves

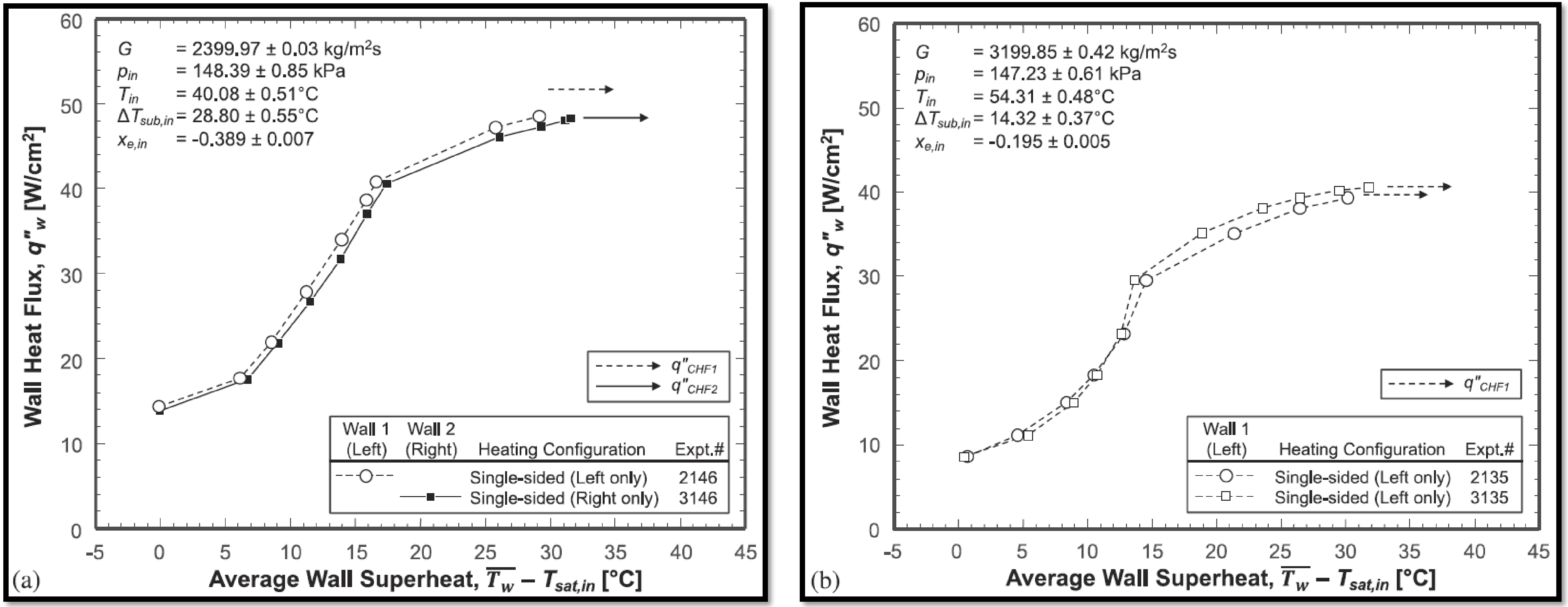

Surface Temperature

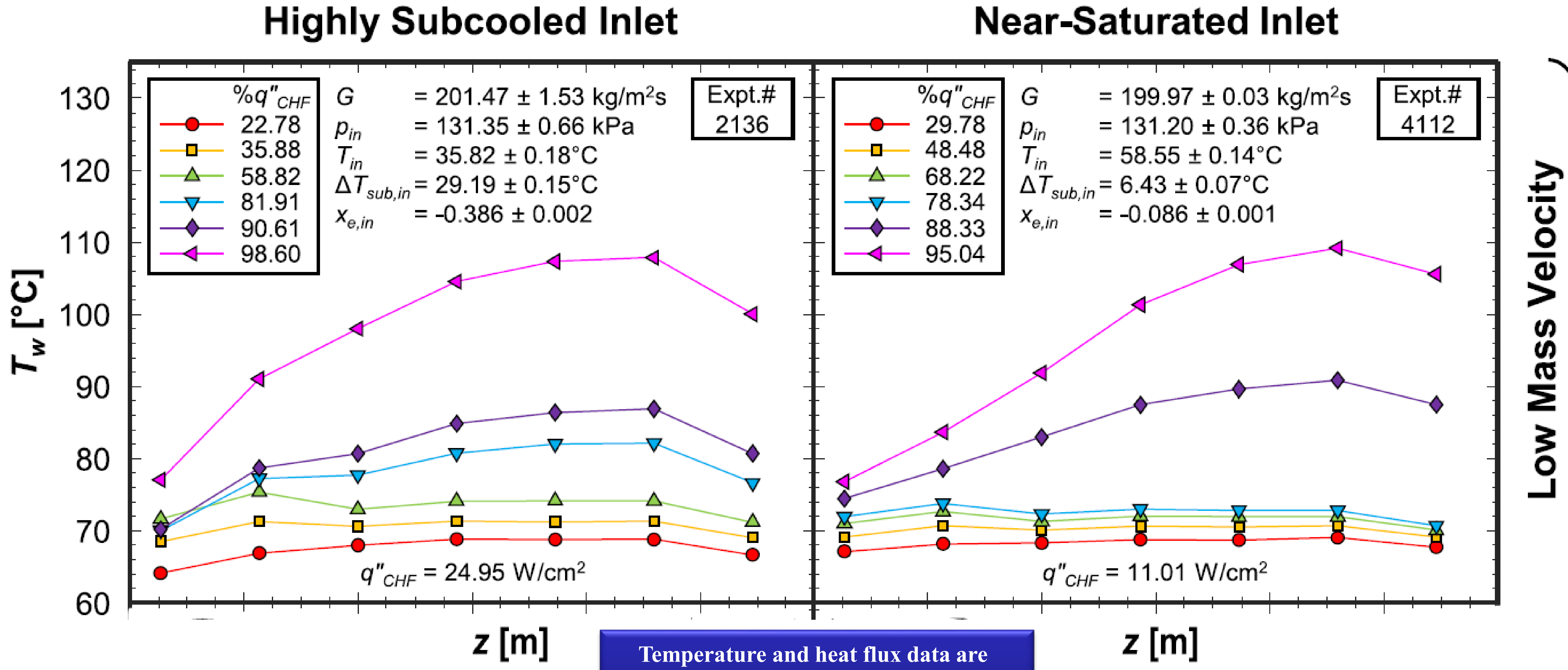

Temperature and heat flux data are combined to calculate the HTC

Local Heat Transfer Coefficient

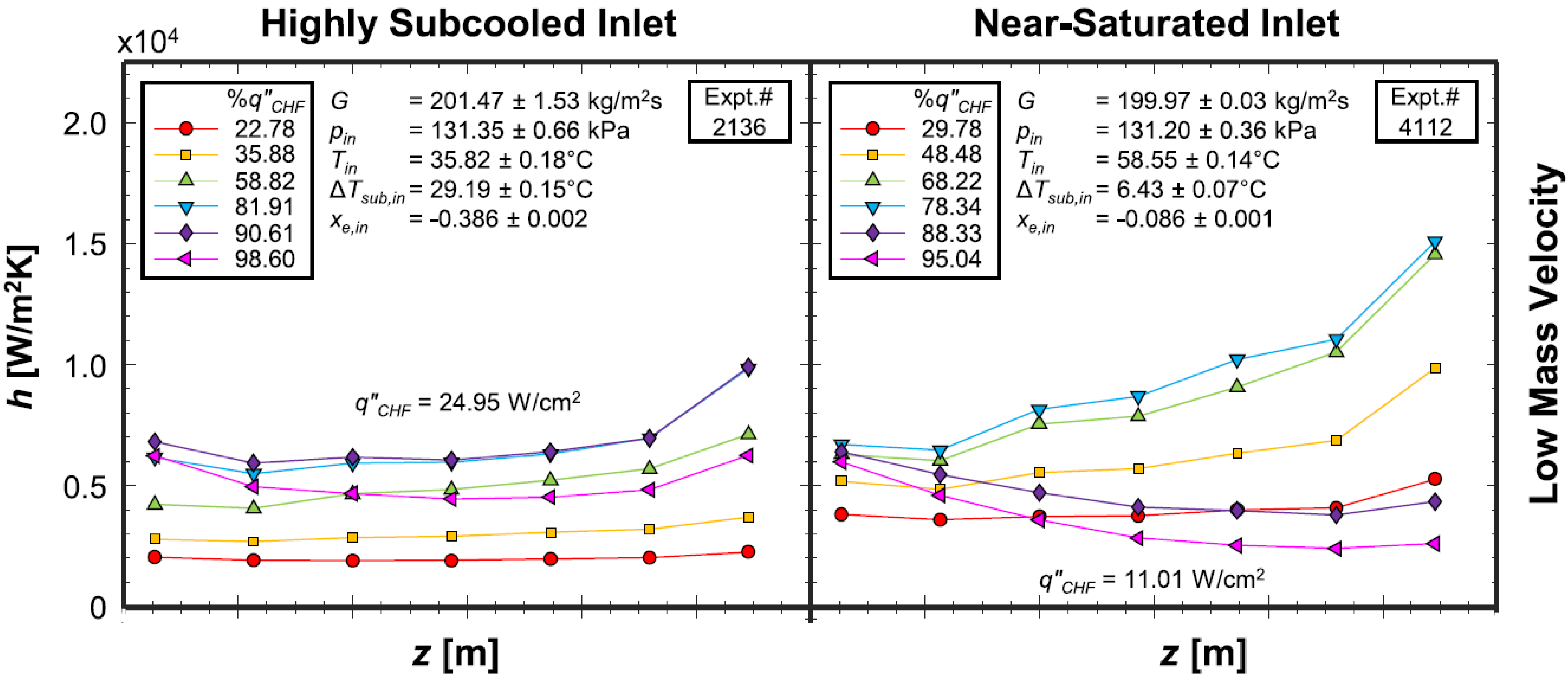

Trends of T_w and h

	High Inlet Subcooling	Low Inlet Subcooling
Local Wall Temperature	▪ T_w is lower along the channel for similar heat fluxes q''	▪ T_w is higher along the channel for similar heat fluxes q''
Heat Transfer Coefficient	▪ Lower heat transfer coefficient ▪ At high heat flux percentages, the upstream part of streamwise *h* profile is not degraded.	▪ Higher heat transfer coefficient ▪ At high heat flux percentages, the entire streamwise *h* profile is severely degraded.
	Low Mass Velocity/Flow Rate	**High Mass Velocity/Flow Rate**
Local Wall Temperature	▪ T_w is higher along the channel for similar heat fluxes q''	▪ T_w is lower along the channel for similar heat fluxes q''
Heat Transfer Coefficient	▪ Lower heat transfer coefficient ▪ Streamwise h profile is decreased at high percentages of CHF	▪ Higher heat transfer coefficient ▪ At high heat flux percentages, *h* profile degradation is limited to the channel middle and exit

Concluding Remarks

- Presented a sample of study areas of flow boiling
  - Imaging
  - Heat Transfer
- Test data is used to generate design correlations that enable calculation of heat transfer coefficient HTC and the Critical Heat Flux CHF in flow boiling
- Imaging and data are used to validate CFD models
- Testing with FBM ended in July
- FBM module will be replaced by the condensation module for heat transfer CM-HT
- Flight testing with CM-HT is planned for September time frame
- Plans to return FBM to Earth and perform a thorough evaluation of the module

References

Heat transfer and interfacial flow physics of microgravity flow boiling in single-side-heated rectangular channel with subcooled inlet conditions – Experiments onboard the International Space Station

Issam Mudawar[a,*], V.S. Devahdhanush[a], Steven J. Darges[a], Mohammad M. Hasan[b], Henry K. Nahra[b], R. Balasubramaniam[c], Jeffrey R. Mackey[d]

[a] Purdue University Boiling and Two-Phase Flow Laboratory (PU-BTPFL), School of Mechanical Engineering, Purdue University, 585 Purdue Mall, West Lafayette, IN 47907, USA
[b] NASA Glenn Research Center, 21000 Brookpark Road, Cleveland, OH 44135, USA
[c] Case Western Reserve University, 10900 Euclid Ave., Cleveland, OH 44106, USA
[d] HX5, LLC 3000 Aerospace Parkway, Brookpark, OH 44142, USA

International Journal of Heat and Mass Transfer 207 (2023) 123998

Experimental results and interfacial lift-off model predictions of critical heat flux for flow boiling with subcooled inlet conditions – In preparation for experiments onboard the International Space Station

Steven J. Darges[a], V.S. Devahdhanush[a], Issam Mudawar[a,*], Henry K. Nahra[b], R. Balasubramaniam[b,c], Mohammad M. Hasan[b], Jeffrey R. Mackey[d]

[a] Purdue University Boiling and Two-Phase Flow Laboratory (PU-BTPFL), School of Mechanical Engineering, Purdue University, 585 Purdue Mall, West Lafayette, IN 47907, USA
[b] NASA Glenn Research Center, 21000 Brookpark Road, Cleveland, OH 44135, USA
[c] Case Western Reserve University, 10900 Euclid Ave., Cleveland, OH 44106, USA
[d] HX5, LLC, 3000 Aerospace Parkway, Brook Park, OH 44142, USA

International Journal of Heat and Mass Transfer 183 (2022) 122241

Experimental heat transfer results and flow visualization of vertical upflow boiling in Earth gravity with subcooled inlet conditions – In preparation for experiments onboard the International Space Station

V.S. Devahdhanush[a], Issam Mudawar[a,*], Henry K. Nahra[b], R. Balasubramaniam[b,c], Mohammad M. Hasan[b], Jeffrey R. Mackey[d]

[a] Purdue University Boiling and Two-Phase Flow Laboratory (PU-BTPFL), School of Mechanical Engineering, Purdue University, 585 Purdue Mall, West Lafayette, IN 47907, USA
[b] NASA Glenn Research Center, 21000 Brookpark Road, Cleveland, OH 44135, USA
[c] Case Western Reserve University, 10900 Euclid Ave, Cleveland, OH 44106, USA
[d] HX5, LLC, 3000 Aerospace Parkway, Brook Park, OH 44142, USA

International Journal of Heat and Mass Transfer 188 (2022) 122603

Flow visualization, heat transfer, and critical heat flux of flow boiling in Earth gravity with saturated liquid-vapor mixture inlet conditions – In preparation for experiments onboard the International Space Station

V.S. Devahdhanush[a], Steven J. Darges[a], Issam Mudawar[a,*], Henry K. Nahra[b], R. Balasubramaniam[b,c], Mohammad M. Hasan[b], Jeffrey R. Mackey[d]

[a] Purdue University Boiling and Two-Phase Flow Laboratory (PU-BTPFL), School of Mechanical Engineering, Purdue University, 585 Purdue Mall, West Lafayette, IN 47907, USA
[b] NASA Glenn Research Center, 21000 Brookpark Road, Cleveland, OH 44135, USA
[c] Case Western Reserve University, 10900 Euclid Ave., Cleveland, OH 44106, USA
[d] HX5, LLC, 3000 Aerospace Parkway, Brook Park, OH 44142, USA

International Journal of Heat and Mass Transfer 192 (2022) 122890

- Thank you for your attention
- Questions?